ACS OMEGA

http://pubs.acs.org/journal/acsodf

Article

Oral Bioavailability-Enhancing and Anti-obesity Effects of Hydroxysafflor Yellow A in Natural Deep Eutectic Solvent

Huan Gao, Hao-Ming Zhou, Shi-Jun Yue,* Li-Mei Feng, Dong-Yan Guo, Jia-Jia Li, Qi Zhao, Lu Huang, and Yu-Ping Tang*

Cite This: *ACS Omega* 2022, 7, 19225−19234

Read Online

ACCESS | Metrics & More | Article Recommendations | Supporting Information

ABSTRACT: Hydroxysafflor yellow A (HSYA), a primary active component in Carthami Flos, has been extensively applied in the treatment of cardiometabolic diseases. In this study, a natural deep eutectic solvent composed of glucose and choline chloride with 10% (v/v) of water (90% GCH) was evaluated to enhance the oral absorption of HSYA. Compared with HSYA in water, the relative oral bioavailability of HSYA in 90% GCH was increased to 326.08%. Furthermore, 90% GCH was demonstrated to decrease the mucus viscosity and increase the absorption rate constant of HSYA in the jejunum by 2.95 times. A pharmacodynamic study revealed that HSYA in 90% GCH was more effective in reducing body weight and correcting steatohepatitis and dyslipidemia in high-fat diet-induced obese rats. Serum metabolomics results showed that the correction of serum aromatic amino acid disorder may contribute to the anti-obesity effect of HSYA in 90% GCH. In conclusion, 90% GCH could be a delivery carrier for HSYA against obesity.

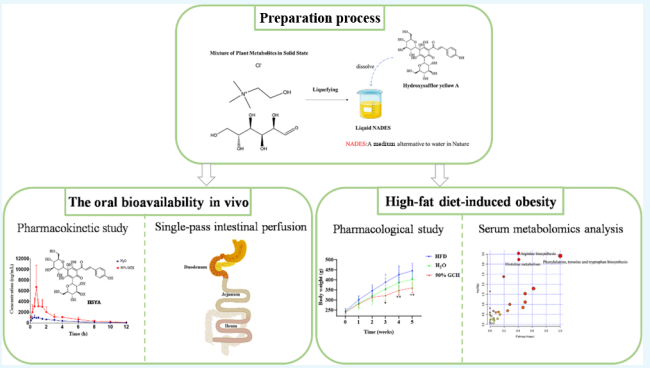

1. INTRODUCTION

Carthamus tinctorius L. belongs to the compositae family and has been used as a food additive and natural pigment for thousands of years. Carthami Flos (the dried florets of *C. tinctorius*) is widely applied for treating cardiometabolic diseases. In Carthami Flos, hydroxysafflor yellow A (HSYA) is a representative water-soluble quinochalcone *C*-glycoside pigment, possessing multiple attractive pharmacological activities against cardiometabolic diseases.[1,2] According to the biopharmaceutics classification system, HSYA belongs to class III drugs with high solubility and low permeability.[3] It has been reported that the oral bioavailability of HSYA in rats was only 1.2% together with a short half-life. Meanwhile, HSYA was highly metabolized in the gastrointestinal tract and liver, resulting in high first-pass extraction, thereby lowering bioavailability.[4,5] In Chinese clinics, safflower yellow injection (HSYA ≥70%, intravenous drip), a yellow pigment extract from Carthami Flos, is one of the top Chinese patent medicines in sales. However, there are still many adverse reactions, such as allergic reactions.[6] It is necessary to design new oral preparation and improve the *in vivo* kinetic behavior of HSYA to make it more effective and safer.

Natural deep eutectic solvents (NADES) are liquid supermolecules formed by natural primary metabolites such as sugars, organic acids, amino acids, and amines as hydrogen bond donors and acceptors through intermolecular interactions, especially hydrogen bonds, and have shown excellent promise in drug delivery applications.[7] Choline-based NADES are emerging as outstanding drug/natural compound carriers due to their biocompatibility, availability, and cost-effectiveness.[8] It has been reported that a NADES composed of glucose and choline chloride with 10% (v/v) of water (90% GCH) was able to stabilize safflower pigments (including HSYA, carthamin, and cartormin) in part due to the strong hydrogen bond interactions between pigments and NADES' molecules.[9,10] Recently, Tong et al. demonstrated that after oral administration of HSYA in L-proline-acetamide (L-Pro-Am), the relative oral bioavailability (Fr, to water extract) of HSYA was 183.5%, suggesting that NADES could be a delivery carrier for HSYA.[11] In our previous study, oral HSYA could reduce body weight and fat accumulation and alleviate insulin resistance in high-fat diet (HFD)-induced obese mice.[12] Solely, choline-based NADES were reported to treat HFD-induced obesity effectively.[13] Therefore, it is intriguing to investigate whether 90% GCH

Received: January 22, 2022
Accepted: May 26, 2022
Published: June 3, 2022

https://doi.org/10.1021/acsomega.2c00457
ACS Omega 2022, 7, 19225−19234

could improve the oral absorption and anti-obesity effects of HSYA.

In this study, the oral bioavailability of HSYA in 90% GCH *in vivo* was evaluated. Second, the effects of H_2O and 90% GCH on intestinal absorption of HSYA were studied by using an *in situ* single-pass intestinal perfusion model. In addition, an HFD-induced obese rat model was employed to evaluate the anti-obesity effect of HSYA in 90% GCH followed by serum metabolomics to explore the potential anti-obesity mechanism. Overall, this work illustrates the promise of using 90% GCH as an oral delivery carrier for HSYA against obesity.

2. MATERIALS AND METHODS

2.1. Chemicals and Materials. Rutin was used as an internal standard (IS, purity: >98.0%) and purchased from Shanghai Yuanye Biotechnology Co., Ltd. (Shanghai, China). D-Glucose, choline chloride, pancreatin, pepsin (from porcine gastric mucosa), and mucin type II were purchased from Sigma (St. Louis, MO, USA). The HFD (D12492, 60% calories from fat) was purchased from Research Diets Inc. (New Brunswick, NJ, USA). Mass spectrum-grade methanol and acetonitrile were purchased from Honeywell Burdick & Jackson (Muskegon, MI, USA). Liquid chromatographic-grade formic acid was obtained from Merck (Darmstadt, Germany). Deionized water was purified using a Millipore Milli-Q system (Bedford, MA, USA). All other reagents and solvents were of analytical grade.

2.2. HSYA Preparation. About 50 g of Carthami Flos was immersed at 60 °C three times in 600 mL of deionized water for 1 h. The water extract was filtered and concentrated at 50 °C under vacuum. The concentrated solution was purified over a column of AB-8 macroreticular resin (Shaanxi Lebo Biochemical Technology Co., Ltd., China), eluted with 0, 30%, 50%, 70%, and 95% ethanol. Furthermore, the 50% eluted part was concentrated and purified by Sephadex LH-20 (GE Healthcare Bio-Sciences AB, Sweden), analyzed in HPLC, and freeze-dried into powder (HSYA purity: >95.0%). By the way, HPLC analysis was performed on a Waters 2695 system equipped with a 2998 PDA detector. A Waters SunFire C18 column (4.6 mm × 150 mm, 5 μm) was used, and the column temperature was set at 25 °C. The mobile phase consisted of methanol (A) and 0.7% phosphate acid water (B). The gradient program was as follows: 10−40% A at 0−2 min, 40−42% A at 2−5 min, 42−45% A at 5−7 min, 45−10% at 7−9 min with a flow rate of 1.0 mL/min. The injection volume was 10 μL, and the wavelength was set at 403 nm.

2.3. 90% GCH Preparation. First, GCH solvent was prepared by mixing glucose and choline chloride at a 2:5 mole ratio with mild heating and stirring at 50 °C. The 90% GCH was prepared by diluting a certain volume with deionized water.

2.4. Solubility Tests. Solubility tests were carried out by saturating solvents (90% GCH and H_2O) with an excess of HSYA in an Eppendorf (EP) tube, stirred at room temperature (20 °C) and 50 °C for 2 h, settled for 3 h, and centrifuged at 12,000 rpm for 20 min. The supernatant was diluted with deionized water and filtrated by 0.22 μm microporous filters. All the samples were tested by triplicate. The HPLC method mentioned in Section 2.2 was used for quantitative analysis of HSYA.

2.5. *In Vivo* Pharmacokinetic Studies. *2.5.1. Instrumentation and Chromatographic Conditions.* Chromatographic analysis was carried out using a Waters ACQUITY I-Class UPLC system (Milford, MA, USA), equipped with a binary pump solvent delivery system, an automatic sampler, and an on-line degasser. A UPLC BEH C18 column (100 mm × 2.1 mm, 1.7 μm) was used for separation. The mobile phase consisted of acetonitrile (A) and water containing 0.1% formic acid (B). The gradient program was as follows: 0.0−1.0 min, 5% A; 1.0−2.5 min, 5−25% A; 2.5−5.0 min, 25−55% A; 5.0−5.5 min, 55−95% A; 5.5−6.0 min, 95−5% A; 6.0−7.5 min, 5% A. The flow rate was 0.30 mL/min. The column temperature and the automatic injector temperature were set at 30 and 10 °C, respectively. MS detection was performed using a Waters Xevo TQ-XS mass spectrometry system (Milford, MA, USA) equipped with an ESI source in negative mode. The ionization source conditions were set as follows: capillary voltage 2.6 kV, desolvation temperature 400 °C, cone gas flow 150 L/h, and desolvation gas flow 1000 L/h. Argon (99.99%) was used as the collision gas. The detection and quantification of the analytes were performed using multiple-reaction monitoring mode. The cone voltage and collision energy were optimized for HSYA (40 and 26 eV) and IS (14 and 34 eV). The dwell time was automatically set by Waters Masslynx v 4.2 software.

2.5.2. Method Validation. Blank plasma samples were obtained from six different male Sprague-Dawley (SD) rats. The chromatogram comparison of blank plasma and blank plasma added with HSYA or IS was used to determine the specificity of assay. The calibration curve of HSYA was based on the ratio of peak area of HSYA to IS and nominal concentration of calibration standards, which was in line with linear regression $y = ax + b$, where x stands for the plasma concentrations of HSYA in rats and y stands for the peak area ratio of HSYA to IS. The range of concentrations of the calibration curve was from 12.5 to 10,000 ng/mL. The lower limit of quantification (LLOQ) was considered as the lowest concentration on the calibration curve with precision variation <20%. Quality control (QC) samples at low, medium, and high concentrations of HSYA were analyzed for three consecutive validation days to assess the intraday and interday precision. The precision and accuracy were expressed as relative standard deviation (RSD) and relative error (RE), respectively. The extraction recovery was used to analyze QC samples with low, medium, and high concentrations of HSYA, which was the ratio of the average peak area of HSYA added before extraction to that after extraction. The stability of QC samples containing low, medium, and high concentrations of HSYA was investigated under the conditions of standing at room temperature for 6 h, repeated freeze−thaw three times, and storage at −20 °C for 6 days.

2.5.3. Pharmacokinetic Study. Ten male SD rats (230−250 g) were provided by Chengdu Dossy Experimental Animals Co., Ltd. (Chengdu, China) and housed in clean plastic cages with free access to water and food in ambient temperature with 40%−60% humidity under a 12 h light and dark cycle for 1 week. These rats were further divided into two groups at random (i.e., the H_2O group and 90% GCH group) and fasted for 12 h with free access to water prior to drug administration. The dosage preparation was made by dissolving appropriate amounts of HSYA in H_2O and 90% GCH (40 mg/mL) and then giving a single dose (100 mg/kg) by gastric gavage. About 300 μL blood samples were immediately collected in heparinized polyethylene tubes at 0.083, 0.25, 0.5, 0.75, 1, 1.5, 2, 3, 4, 6, 8, 10, and 12 h after dosing from the fossa orbitalis vein of the rats in both groups. After centrifugation at 5000 rpm for 10 min, plasma was finally obtained and stored at −80 °C until analysis. The animal welfare and experimental procedures were strictly in accordance with the guide for the Care and Use of Laboratory Animals (US National Research Council, 1996) and the related ethics

https://doi.org/10.1021/acsomega.2c00457
ACS Omega 2022, 7, 19225−19234

regulations of the Ethical Committee of Shaanxi University of Chinese Medicine.

2.5.4. Sample Preparation. A 100 μL plasma sample was added with 10 μL of IS and 190 μL of methanol in a 1.5 mL EP tube. The mixture was vortexed for 30 s and then centrifuged at 14,000 rpm for 10 min. The supernatant was transferred to a fresh 1.5 mL EP tube and centrifuged at 14,000 rpm for another 10 min. At last, 1.5 μL of the supernatant was injected for UPLC-MS/MS analysis.

2.5.5. Pharmacokinetic Parameter Calculation. To determine the pharmacokinetic parameters, concentration−time data were analyzed with a non-compartmental method using DAS 2.0 software. The maximum plasma concentration (C_{max}) and peak time (T_{max}) of HSYA were determined directly from the mean plasma concentration−time ($C-T$) curve. The areas under the $C-T$ curve from time 0 to t (AUC_{0-t}) and from time 0 to infinity ($AUC_{0-\infty}$) were calculated using the linear trapezoidal rule. The terminal half-life ($t_{1/2}$) was calculated as 0.693/kel, where kel was the apparent elimination rate constant of HSYA from plasma. The AUC_{0-t} of HSYA in 90% GCH versus H_2O was used to calculate the relative bioavailability (Fr).

2.6. Mucus Rheology Studies. The biological similarity mucus was modified on a previously reported method.[14] Specifically, 0.75% (w/v) polysorbate 80 was added to 0.5% carboxymethylcellulose sodium and 5% mucus was added to make simulated mucus under stirring conditions. A total of 10 μL of 0, 3.13, 6.25, 12.5, 25, and 50% v/v of 90% GCH was added to 200 μL of simulated mucus, and viscosity was measured with a rheometer in the shear rate range of 1−200 1/s at 37 °C.

2.7. *In Situ* Single-Pass Intestinal Perfusion. It has been reported that HSYA is mainly absorbed in small intestinal segments.[15] Herein, the effects of 90% GCH on the absorption of HSYA in small intestinal segments (i.e., duodenum, jejunum, and ileum) were studied. The male SD rats were divided into two groups ($n = 3$). Before the operation, the rats were fasted for 12 h and free to drink water. The preparation of Krebs-Ringer (K-R) buffer was done according to a previous literature study.[16] Rats were anesthetized with 10% (v/w) chloral hydrate, and normal body temperature was maintained with an infrared lamp. After confirming the disappearance of pain reflex, the duodenum, jejunum, and ileum (approximately 10 cm) were carefully pulled out and small cuts were made at the beginning and the end, and silicone tubes were inserted and ligated. The inlet was filled with a well-weighed EP tube equipped with a test solution, and another well-weighed EP tube was placed at the exit to collect the effluent. After the operation, cotton pads soaked in saline were used to cover the wound. The intestinal contents were rinsed with normal saline, and the preheated K-R buffer and a drug-containing perfusate were equilibrated at 37 °C for 30 min at a flow rate of 0.2 mL/min. After 30 min balance, a 5 mL EP tube with known weight containing 1 mg/mL HSYA in H_2O or 90% GCH was immediately used for intestinal perfusion. A 5 mL EP tube with known weight was used to receive the effluent at the exit and was replaced every 15 min for a total of 90 min. At the end, the perfused intestinal segments were cut off. The length and circumference of the intestinal segments were measured under normal saline at 4 °C to ensure that the intestinal segment was not stretched.

For the determination of HSYA, 500 μL of the effluent was taken, added with 500 μL of methanol, and centrifuged at 12,000 rpm under 4 °C for 10 min. Finally, 10 μL of the supernatant was injected for HPLC analysis according to the method mentioned in Section 2.2.

The absorption rate constant (K_a), the effective permeability coefficient (P_{eff}), and the absorption percentage (F_{ab}) of HSYA in the small intestine were calculated according to the following mathematical expression:[17,18]

$$C_{out(corrected)} = C_{out}\frac{V_{out}}{V_{in}} \quad (1)$$

$$K_a = \left[1 - \frac{C_{out(corrected)}}{C_{in}}\right] Q/\pi r^2 L \quad (2)$$

$$P_{eff} = -\frac{Q}{2\pi rL}\ln\left[\frac{C_{out(corrected)}}{C_{in}}\right] \quad (3)$$

$$F_{ab} = Qt(C_{in} - C_{out(corrected)}) \quad (4)$$

where V_{in} and V_{out} are the volumes of the perfusate entering and leaving the intestine, respectively; Q is the perfusion flow rate; C_{in} and C_{out} are the concentration of the drug in the perfused inlet and outlet, respectively; L is the length of the intestinal segment (cm), and r is the radius of the intestinal segment (cm).

2.8. Stability Study in Simulated Gastric and Intestinal Juices. The simulated gastric and intestinal juices were prepared according to Chinese Pharmacopeia.[19] HSYA (1 mg/mL) in H_2O and 90% GCH was added to simulated gastric and intestinal juices (v/v, 1:7.5) and incubated at 37 °C for 0, 1, 2, or 4 h, respectively. The juice (200 μL) was sampled at each time point and centrifuged at 12,000 rpm for 10 min. Finally, 10 μL of supernatant was injected for HPLC analysis according to the method mentioned in Section 2.2.

2.9. Pharmacological Study. *2.9.1. Animals and Experimental Design.* The male SD rats were divided into three groups ($n = 6$) and fed with an HFD (D12492, 60% calories from fat) for 5 weeks. Two of the groups were orally dosed daily for 5 weeks with 100 mg/kg HSYA in H_2O and 90% GCH. The other group of rats was treated with pure water. Throughout the trial, the body weight was recorded weekly. All experiments were terminated at the end of the fifth week.

2.9.2. Oral Glucose Tolerance Test (OGTT). After a 6 h fasting period, blood glucose was determined with a glucose meter (Abbott FreeStyle Optium, Witney, UK) using the blood collected from the tip of the tail vein before and 30, 60, 90, and 120 min after D-glucose (2.0 g/kg, 50% solution; Hubei Kelun Pharmaceutical Co., LTD.) challenge. Cumulative changes in blood glucose response were quantified by the incremental area under the curve (AUC).

2.9.3. Collection of Serum and Tissue Samples. At the end of the fifth week, fasting for 12 h was performed under 10% chloral hydrate anesthesia and 4 mL blood samples were taken from the abdominal aorta. Blood was centrifuged at 3000 rpm for 10 min under 4 °C. Then, the serum samples were collected and stored at −80 °C. The epididymal fat, liver, stomach, duodenum, jejunum, ileum, lung, spleen, heart, and kidney of each rat were immediately excised, and the liver was weighed. All samples were stored in 4% paraformaldehyde for follow-up analysis. The liver index was calculated as a percentage of liver weight to body weight.

2.9.4. Biochemical Measurements. Alanine aminotransferase (ALT), aspartate transaminase (AST), blood urea nitrogen (BUN), creatinine, total triglycerides (TG), high-density

https://doi.org/10.1021/acsomega.2c00457
ACS Omega 2022, 7, 19225−19234

lipoprotein cholesterol (HDL), and low-density lipoprotein cholesterol (LDL) were measured using kits for rats from Royta life and Analytical Sciences, Shenzhen, China. Serum total cholesterol (TC) and fasting serum glucose (GLU) were measured using kits for rats from Nanjing Jiancheng Bioengineering Institute, Nanjing, China. All kits were used according to the manufacturers' instructions.

2.9.5. Histopathological Analysis. Tissue samples were fixed in 4% paraformaldehyde for 24 h and embedded in paraffin. Tissues were cut into sections (each 4 μm-thick) and stained using hematoxylin and eosin (H&E). Histological sections were analyzed and photographed under a light microscope (Nikon Eclipse E100, Nikon, Japan).

2.10. Serum Metabolomics Analysis. *2.10.1. Instrumentation and Chromatographic Conditions.* UHPLC−MS/MS analysis was performed using a Vanquish UHPLC system (Thermo Fisher, Germany) coupled with an Orbitrap Q Exactive HF mass spectrometer (Thermo Fisher, Germany). Serum samples were separated on a Hypesil Gold C18 column (100 × 2.1 mm, 1.9 μm, Thermo Fisher, Germany) using methanol (A) and water containing 0.1% formic acid (B) as the mobile phase for positive mode and methanol (A) and 5 mM ammonium acetate (B, pH 9.0) as the mobile phase for negative mode. The gradient elution was optimized as follows: 0.0−1.5 min, 2% A; 1.5−12.0 min, 2−100% A; 12.0−14.0 min, 100% A; 14.0−14.1 min, 100−2% A; 14.1−17.0 min, 2% A. The column temperature was 40 °C, and the flow rate was 0.20 mL/min. The ionization source conditions were set as follows: spray voltage 3.2 kV, capillary temperature 320 °C, sheath gas flow rate 40 arb, and aux gas flow rate 10 arb.

2.10.2. Sample Preparation. Serum (100 μL) was placed in a 1.5 mL EP tube and fully vortexed with precooled 400 μL of 80% methanol. Then, the sample was incubated on ice for 5 min and centrifuged at 15,000*g* at 4 °C for 20 min. The supernatant (400 μL) was diluted to final concentration containing 53% methanol and then transferred to a fresh 1.5 mL EP tube and centrifuged at 15,000*g* at 4 °C for 20 min. The final supernatant was injected for UHPLC−MS/MS analysis.

2.10.3. Data Processing and Analysis. The raw MS files were processed using Compound Discoverer 3.1 (CD 3.1, ThermoFisher). Peak intensities were normalized to the total spectral intensity. The normalized data was used to predict the molecular formula based on additive ions, molecular ion peaks, and fragment ions. Then, the peaks were matched with the mzCloud (https://www.mzcloud.org/), mzVault, and MassList databases to obtain the accurate qualitative and relative quantitative results. Metabolites were annotated using the KEGG (https://www.genome.jp/kegg/pathway.html), HMDB (https://hmdb.ca/metabolites), and LIPIDMaps (http://www.lipidmaps.org/) databases. Principal component analysis (PCA) and partial least squares discriminant analysis (PLS-DA) were performed at metaX (BGI Tech, China). *T*-tests were used to calculate the statistical significance (*P*-value). The metabolites with variable importance in projection (VIP) > 1 and *P*-value < 0.05 as well as fold change (FC) > 1.2 or FC < 0.833 were considered to be differential metabolites. Pathway analysis was performed with the MetaboAnalyst 5.0 pathway analysis module (http://www.metaboanalyst.ca).

2.11. Statistical Analysis. Experimental data were analyzed using SPSS 25.0. Differences between multiple groups were analyzed using one-way ANOVA with Tukey's multiple comparisons test. For comparisons between two groups, Student's *t*-tests were used for parametrically distributed data and Mann−Whitney tests for nonparametrically distributed data. All data were presented as mean ± SD. When $P < 0.05$, it was considered statistically significant.

3. RESULTS

3.1. HSYA Solubility in H_2O and 90% GCH. The solubilities of HSYA in H_2O were 258.814 ± 14.519 mg/mL at 20 °C and 321.877 ± 6.756 mg/mL at 50 °C. Due to the high viscosity of 90% GCH, the solubilities of HSYA were reduced to 153.254 ± 7.054 mg/mL at 20 °C and 176.550 ± 7.921 mg/mL at 50 °C.

3.2. 90% GCH Enhanced the Oral Bioavailability of HSYA. With the aim of investigating if 90% GCH could increase the oral bioavailability of HSYA, we established and validated a UPLC-MS/MS method to determine the plasma concentration of HSYA. The retention times of HSYA and IS were 3.03 and 3.51 min, respectively, with no observed endogenous interference (Figure 1A). The calibration curve for HSYA was y =

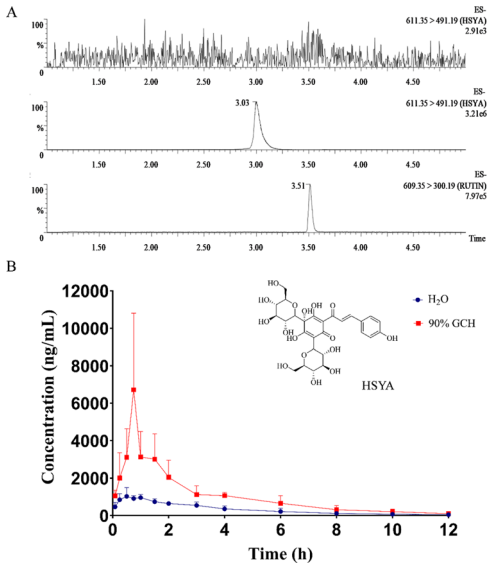

Figure 1. Effect of 90% GCH on the oral bioavailability of HSYA. (A) Typical mass spectrograms of blank plasma and plasma spiked with HSYA and rutin. (B) Time course of plasma concentrations of HSYA in rats. The data is shown as mean ± SD (n = 5).

0.00150532x − 0.0126754, with r^2 = 0.9992. The LLOQ for HSYA was regarded as 12.5 ng/mL. The average extraction recoveries were ranged from 93.1 to 104.9%, while the average matrix effects were between 93.7 and 102.2% (Table S1 in the Supporting Information), indicating that the pretreatment method was appropriate. The intra- and interday precision variations of HSYA at each QC level were within 1.7−6.4%. The RE of accuracy was within ±5.7% (Table S2 in the Supporting Information). The stability of HSYA was acceptable at room temperature for 6 h, three freeze−thaw cycles, and at −20 °C for 6 days. All RSD values were less than 14.3%, and RE values were within ±9.9% (Table S3 in the Supporting Information). These results indicated that the developed UPLC-MS/MS method is satisfactory to determine the plasma HSYA concentration.

The $C-T$ curves of HSYA in H_2O and 90% GCH groups are shown in Figure 1B. Meanwhile, the major pharmacokinetic parameters are listed in Table 1. Specifically, HSYA in both groups was absorbed rapidly and reached C_{max} within 1 h and then eliminated in 12 h. Nevertheless, the C_{max} of HSYA in the

https://doi.org/10.1021/acsomega.2c00457
ACS Omega 2022, 7, 19225−19234

Table 1. Main Pharmacokinetic Parameters of HSYA in Rats (n = 5)[a]

		HSYA	
parameter	unit	H_2O group	90% GCH group
$AUC_{(0-t)}$	ng·h/mL	3853.07 ± 518.39	12564.13 ± 4198.50**
$AUC_{(0-\infty)}$	ng·h/mL	4186.25 ± 534.01	13242.62 ± 4052.52**
$T_{1/2}$	h	4.12 ± 1.49	3.18 ± 1.22
C_{max}	ng/mL	1177.83 ± 389.32	5912.00 ± 3973.30**
T_{max}	h	0.80 ± 0.48	1.00 ± 0.56

[a]The data is shown as mean ± SD. *P < 0.05, **P < 0.01, compared with the H_2O group.

90% GCH group was 5.02-fold as that in the H_2O group. The AUC values were also significantly increased (P < 0.05), resulting in the Fr of HSYA in 90% GCH at 326.08%.

3.3. 90% GCH Decreased the Simulated Mucus Viscosity. The mucus barrier lining the gastrointestinal tract poses a significant barrier to drugs' oral delivery,[20] so the rheology of simulated mucus treated with 90% GCH was assessed. The viscosity of the simulated mucus treated with 90% GCH showed a notable drop throughout the entire measured shear range. At a shear rate of 50 1/s, the mean viscosity of untreated simulated mucus was measured as 10.07 mpa·s. The addition of 3.13, 6.25, 12.5, 25, and 50% v/v of 90% GCH decreased the mean simulated mucus viscosity to 9.08, 8.03, 8.93, 9.02, and 8.34 mpa·s, respectively, with the minimum corresponding to 6.25% v/v of 90% GCH.

3.4. 90% GCH Increased Small Intestinal Absorption of HSYA *In Situ*. The small intestine is the primary site of drug absorption in the gastrointestinal tract. The *in situ* single-pass intestinal perfusion model was used to explore the effects of H_2O and 90% GCH on the small intestinal absorption of HSYA. As shown in Table 2, K_a values in the jejunum were 2.95 times higher than that in the H_2O group. Meanwhile, the P_{eff} and F_{ab} values of jejunum and ileum increased significantly (P < 0.05). Surprisingly, the P_{eff} and K_a values of jejunum in 90% GCH group were significantly higher than those of duodenum and ileum (P < 0.05).

3.5. 90% GCH Increased the Stability of HSYA in Simulated Gastric and Intestinal Juices. We also considered whether 90% GCH could prevent HSYA degradation from gastric and intestinal juices. In Table 3, HSYA in both groups in simulated intestinal juice was more stable than simulated gastric juice. In simulated gastric juice, the degradation of HSYA in 90% GCH was slower than that in the H_2O group within 1−2 h. The degradation of HSYA in 90% GCH in simulated gastrointestinal (gastric × intestinal) juice within 2 h was slower than that in the H_2O group but increased rapidly on 4 h.

3.6. 90% GCH Enhanced the Protective Effect of HSYA against HFD-Induced Obesity. The average body weight and liver index of rats in the 90% GCH group was significantly decreased compared with the HFD group (Figure 2A,C, P < 0.05 or P < 0.01). Meanwhile, the rats in the 90% GCH group ate less food than HFD-fed rats (Figure 2B). The AUC of OGTT was significantly decreased in the 90% GCH group compared with H_2O and HFD groups (Figure 2D,E, P < 0.05 or P < 0.01), suggesting that 90% GCH could reinforce the positive effect of HSYA on impaired glucose tolerance induced by HFD. The following serum biochemical indicators were also measured: ALT, AST, BUN, Creatinine, GLU, TC, TG, HDL, and LDL (Figure 2F−N). Among them, AST in the 90% GCH group was significantly lower than that in the other two groups (Figure 2G, P < 0.05), indicating that 90% GCH may strengthen the effect of HSYA on steatohepatitis induced by HFD. In addition, HDL in the 90% GCH group was higher than that in the other two groups (Figure 2M, P < 0.05 or P < 0.01), whereas LDL in the 90% GCH group was lower than that in the other two groups (Figure 2N, P < 0.05). These results revealed that 90% GCH could improve the treatment effect of HSYA on dyslipidemia. No significant differences in serum ALT, BUN, Creatinine, GLU, TC, and TG levels were observed among the three groups. Moreover, the 90% GCH group reduced the epididymal fat area and liver lipid droplet size compared with the HFD group. No morphological abnormalities were observed in the stomach, duodenum, jejunum, and ileum, indicating that 90% GCH did not impact the native mucus gel structure. Also, H&E staining images of the lung, spleen, heart, and kidney were identical in all groups (Figure S1). Above all, 90% GCH could effectively and safely enhance the treatment effect of HSYA against HFD-induced obesity.

We further analyzed the perturbation of endogenous serum metabolites using UHPLC−MS/MS. PCA analysis showed that the QC samples were clustered, suggesting that the experimental data were well controlled. The metabolic pattern of the 90% GCH group tended to be separate from that of the HFD group and H_2O group (Figure 3A). The PCA and PLS-DA analysis were further performed in the HFD group and 90% GCH group,

Table 3. Stability of HSYA in Simulated Gastric and Intestinal Juices at Different Times (n = 3)[a]

	simulated gastric juice (%)		simulated intestinal juice (%)		simulated gastrointestinal juice (%)	
time (h)	H_2O group	90% GCH group	H_2O group	90% GCH group	H_2O group	90% GCH group
0	100	100	100	100	100	100
1	97.186 ± 2.110	97.665 ± 1.377	98.126 ± 1.457	99.841 ± 1.899	95.361 ± 2.286	97.494 ± 0.787
2	92.671 ± 2.619	96.149 ± 1.984	97.091 ± 3.104	97.802 ± 1.210	90.021 ± 5.248	94.052 ± 3.109
4	89.195 ± 3.213	90.816 ± 0.379[#]	94.091 ± 3.522*	96.595 ± 0.620*	85.268 ± 5.299	87.725 ± 0.917

[a]The data is shown as mean ± SD; *P < 0.05, compared with the same group in simulated gastric juice; [#]P < 0.05, compared with the 90% GCH group in simulated gastric juice on the second hour.

Table 2. Absorption Parameters of HSYA in Different Segments of the Rat Small Intestine (n = 3)[a]

	P_{eff} (×10^{-5}) (cm·s^{-1})		K_a (×10^{-3}) (s^{-1})		F_{ab} (%)	
intestine segment	H_2O group	90% GCH group	H_2O group	90% GCH group	H_2O group	90% GCH group
duodenum	1.973 ± 0.451	2.634 ± 0.522[#]	0.229 ± 0.040	0.342 ± 0.008*[#]	17.884 ± 1.460	21.490 ± 4.159
jejunum	1.588 ± 0.275	4.489 ± 0.507*	0.174 ± 0.031	0.514 ± 0.097*	11.693 ± 0.671	22.761 ± 2.693*
ileum	1.958 ± 0.595	3.254 ± 0.342*[#]	0.216 ± 0.064	0.360 ± 0.025*[#]	12.364 ± 3.510	21.929 ± 1.299*

[a]The data is shown as mean ± SD; *P < 0.05, compared with the H_2O group; [#]P < 0.05, compared with jejunum.

https://doi.org/10.1021/acsomega.2c00457
ACS Omega 2022, 7, 19225−19234

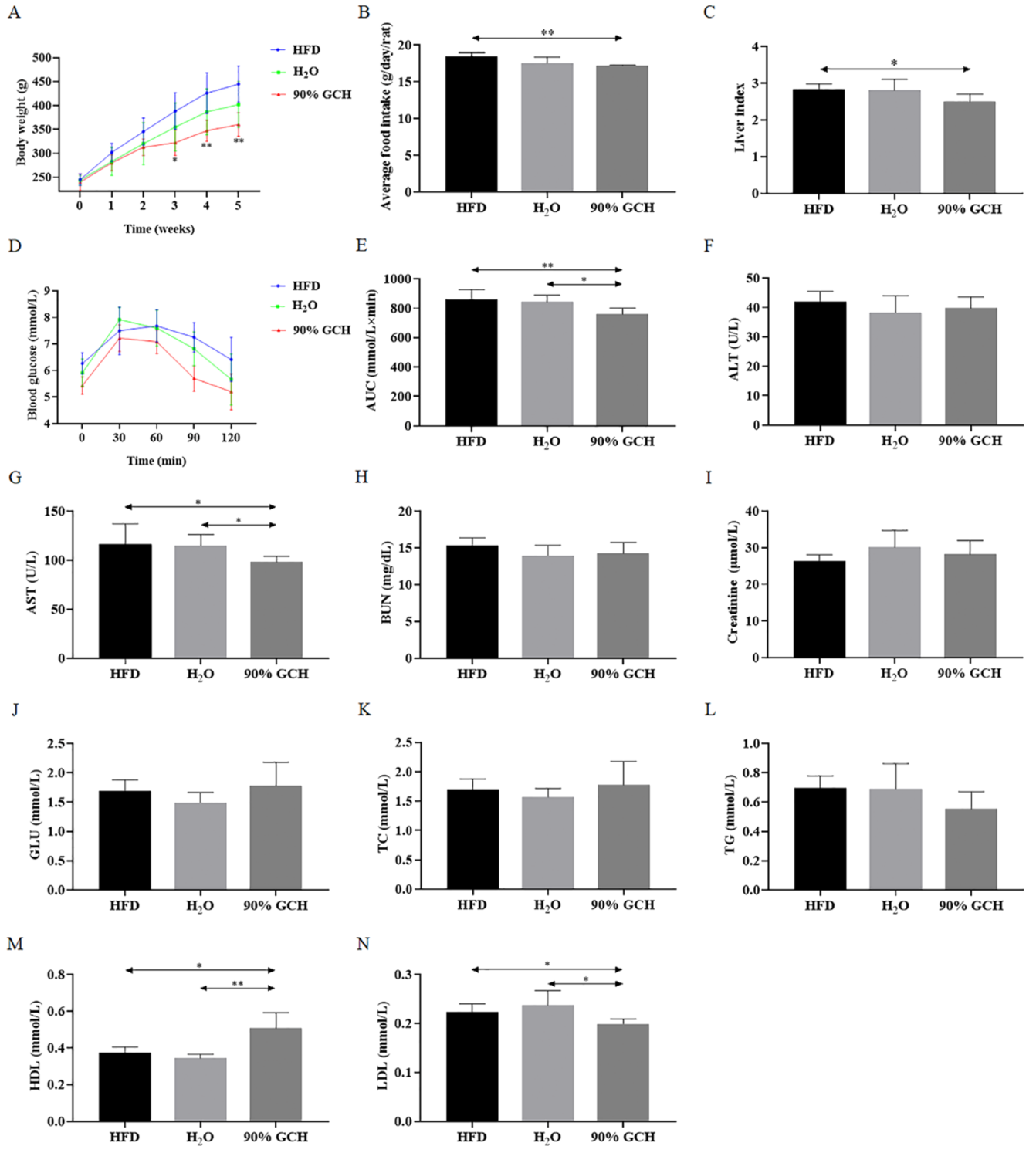

Figure 2. Effects of 90% GCH on HSYA against HFD-induced obesity. (A) Body weight. (B) Food intake. (C) Liver index. (D) Oral glucose tolerance test (OGTT) curves. (E) Area under the curve (AUC) of OGTT. (F) Serum alanine aminotransferase (ALT). (G) Serum aspartate aminotransferase (AST). (H) Blood urea nitrogen (BUN). (I) Creatinine. (J) Fasting serum glucose (GLU). (K) Serum total cholesterol (TC). (L) Serum total triglycerides (TG). (M) High-density lipoprotein cholesterol (HDL). (N) Low-density lipoprotein cholesterol (LDL). The data is shown as mean ± SD ($n = 6$). *$P < 0.05$, **$P < 0.01$.

and the metabolic patterns of the two groups were also significantly different (Figure 3B,C). Subsequently, we screened the differential metabolites by VIP > 1, FC > 1.2 or FC < 0.833, and P value < 0.05. A total of 61 potential differential metabolites were identified between H_2O and HFD groups (Figure 3D). Importantly, compared with the HFD group, 90 increased metabolites and 129 decreased metabolites were identified in the 90% GCH group (Figure 3E). The detailed information is shown in Table S4 of the Supporting Information. Hierarchical clustering analysis results showed that the metabolic patterns in HFD and 90% GCH groups were reversed (Figure 3F). The metabolic pathway analysis further confirmed that arginine

https://doi.org/10.1021/acsomega.2c00457
ACS Omega 2022, 7, 19225−19234

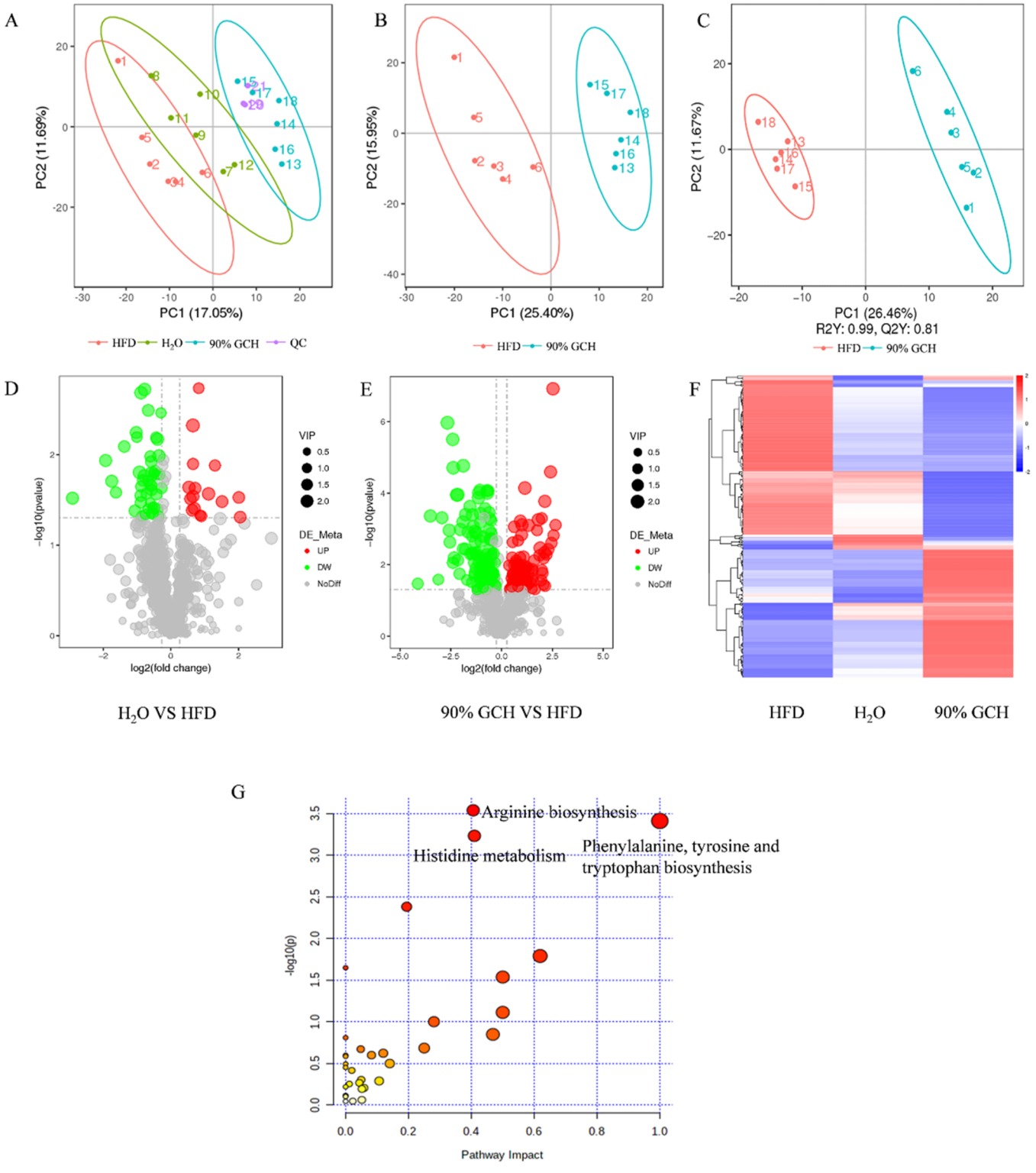

Figure 3. Effects of HSYA in 90% GCH on serum metabolites against HFD-induced obesity. (A) PCA score plot of the three groups and QC samples. (B) PCA score plot (group HFD vs 90% GCH). (C) PLS-DA score plot (group HFD vs 90% GCH). Volcano plots of differential metabolites (D) between groups H_2O and HFD and (E) between groups 90% GCH and HFD. (F) Hierarchical clustering analysis of differential metabolites among the three groups. (G) Pathway analysis of metabolic variations with MetPA.

biosynthesis, phenylalanine, tyrosine, and tryptophan biosynthesis, and histidine metabolism were the top three enrichment and topological pathways involved in the treatment of HSYA in 90% GCH (Figure 3G).

4. DISCUSSION

The oral bioavailability of HSYA is extremely low, mainly due to its good water solubility and poor lipid solubility, which made it difficult to penetrate the intestinal mucosa. Considering the good biocompatibility of choline-based NADES, 90% GCH was

https://doi.org/10.1021/acsomega.2c00457
ACS Omega 2022, 7, 19225−19234

evaluated to enhance oral absorption of HSYA. *In vivo* pharmacokinetic results showed that 90% GCH significantly increased the oral absorption of HSYA in rats with an Fr at 326.08%. 90% GCH could affect not only the absorption rate constant but also the extent of absorption. The AUC values in the 90% GCH group were significantly increased compared with the H_2O group, indicating that 90% GCH promoted the absorption extent of HSYA. Compared with the L-Pro-Am solvent,[11] the oral bioavailability of HSYA in 90% GCH was increased by 1.78 times, suggesting that 90% GCH was more effective. L-Proline is a non-essential amino acid of protein synthesis in the human body, whereas acetamide is clinically used for organic fluorine pesticide poisoning and belongs to class 2B carcinogen. Although Tong et al. reported L-Pro-Am as a drug delivery vehicle, its safety remains to be studied.[11] 90% GCH is composed of choline chloride and glucose. Choline chloride can be used in the treatment of fatty liver and cirrhosis and as a feed additive. The content of choline in 90% GCH is lower than those used in dietary supplements. Therefore, we do not anticipate choline in 90% GCH to produce any significant biological effects. At the same time, our study demonstrated that 90% GCH is non-toxic and has good biocompatibility during the experiment. A previous study has reported that choline chloride-based NADES are eco-friendly, non-toxic, and biodegradable organic compounds, which maintain the biological activity of the target compound and are currently one of the most studied NADES in drug delivery applications.[21] Moreover, glucose and choline chloride have more hydroxyl groups, which provide strong stabilization ability originating from the formation of strong hydrogen bonding interactions between HSYA and themselves.[22] In addition, the viscosity of the simulated mucus treated with 90% GCH showed a notable drop throughout the entire measured shear range, suggesting that 90% GCH could be a potential mucus-modulating agent for improving the mucus penetration of HSYA. The *in situ* single-pass intestinal perfusion experiment further confirmed that the absorption rate constant of HSYA in the jejunum of the 90% GCH group was increased by 2.95 times, thereby increasing the oral absorption of HSYA. Consistent with the pharmacokinetic results, the stability experiments showed that the degradation of HSYA in 90% GCH in the simulated gastrointestinal juice within 2 h was slower than that in the H_2O group, which may partially contribute to the high blood concentration maintained within 2 h. Previous studies demonstrated that choline-based NADES reduced mucus viscosity without significantly impacting the native mucus gel structure, suggesting that it would assist in mucus penetration *in vivo*.[8,23] Based on this information and our data, we believe that 90% GCH protects HSYA from enzymatic degradation, assists in the transport of HSYA through the mucous layer, and mediates the penetration of HSYA through the intestinal mucosa and increases the drug concentration into the blood. In addition, the absorption of HSYA is affected by the efflux transporter such as P-gp and BCRP in intestinal epithelial cells, which is also an important reason for the low bioavailability of HSYA.[15] Moreover, the intestinal flora is rich in enzyme systems, which participate in the catabolic process of HSYA *in vivo*.[24,25] The high viscosity of 90% GCH may protect HSYA from intestinal flora metabolism and lead to its increased oral bioavailability, but more evidence is needed.

Based on serum biochemical and multiorgan histological analyses, HSYA in 90% GCH was more effective in alleviating body weight, steatohepatitis, and dyslidemia in obese rats, and no morphological abnormalities were observed in any other tissues. Therefore, we do not anticipate choline in 90% GCH to produce any significant biological effects, although additional studies are needed to fully understand the potential role of 90% GCH. The mechanism findings based on serum metabolomics revealed that the major metabolites affected by HSYA in 90% GCH were related to amino acid metabolism, which is closely related to obesity.[26] Generally, amino acids serve as the basic constituents of proteins and can also enter the tricarboxylic acid cycle through transamination or oxidative deamination to provide energy when glucose and lipids cannot be effectively utilized in diabetic or insulin-resistant states.[27] High levels of aromatic amino acids (AAA) are known risk factors for obesity and cardiometabolic diseases, which refers to phenylalanine, tyrosine, and tryptophan. Phenylalanine is a metabolic precursor to tyrosine *via* phenylalanine hydroxylase in the liver, which further metabolizes to neurotransmitters.[28] L-Tyrosine is one of the amino acids believed to be related to body mass index and is positively correlated with obesity in humans, and its level has been shown to decrease after weight loss.[29] Tryptophan is generally degraded by the kynurenine pathway.[30] AAA could convert to phenylpyruvic acid, 4-hydroxyphenylpyruvic acid, and indole-3-pyruvic acid by AAA aminotransaminase-mediated transamination.[31] In addition, tryptophan is also degraded and metabolized by gut bacteria into 3-methylindoles.[32] In this study, after HSYA in 90% GCH intervention, AAA and their metabolites, i.e., L-tyrosine, phenylpyruvic acid, and 3-methylindoles were significantly decreased in obese rats. Moreover, histidine is an important amino acid in the body, which can be utilized to produce glucose through gluconeogenesis.[33] Thus, changes in histidine metabolism may lead to an imbalance of energy and glucose homeostasis. A recent study reported that obese individuals have a rich histidine metabolism.[34] Collectively, HSYA in 90% GCH can partially correct the amino acid metabolism disorders in HFD-induced obesity.

5. CONCLUSIONS

In this study, 90% GCH was developed to increase the oral bioavailability of HSYA *in vivo* with an Fr at 326.08%. The viscosity of the 90% GCH-treated simulated mucus was decreased significantly. Further analysis by *in situ* intestinal perfusion showed that 90% GCH significantly enhanced the small intestinal absorption rate constant of HSYA, in which the jejunum absorption rate was increased by about 2.95 times. The pharmacodynamic results showed that HSYA in 90% GCH effectively and safely attenuated steatohepatitis, corrected blood lipids, and improved glucose intolerance induced by HFD. Serum metabolite spectrum and pathway enrichment analysis revealed that HSYA in 90% GCH could partially restore the disorder of amino acid metabolism. In conclusion, our findings suggest that 90% GCH could be a promising oral drug delivery carrier for HSYA against cardiometabolic diseases.

■ ASSOCIATED CONTENT

Supporting Information

The Supporting Information is available free of charge at https://pubs.acs.org/doi/10.1021/acsomega.2c00457.

Matrix effect of HSYA and rutin (IS) in rat plasma (Table S1); precision, accuracy, and recovery for the analysis of HSYA in rat plasma (Table S2); stability of HSYA in rat plasma (Table S3); differential metabolites in serum samples between 90% GCH and HFD groups (Table S4); and representative hematoxylin and eosin staining images

https://doi.org/10.1021/acsomega.2c00457
ACS Omega 2022, 7, 19225−19234

of the epididymal fat, liver, stomach, duodenum, jejunum, ileum, lung, spleen, heart, and kidney in different groups (Figure S1) (PDF)

AUTHOR INFORMATION

Corresponding Authors

Shi-Jun Yue − *Key Laboratory of Shaanxi Administration of Traditional Chinese Medicine for TCM Compatibility, Shaanxi University of Chinese Medicine, Xi'an 712046, China;* orcid.org/0000-0003-2097-223X; Email: shijun_yue@163.com

Yu-Ping Tang − *Key Laboratory of Shaanxi Administration of Traditional Chinese Medicine for TCM Compatibility and State Key Laboratory of Research & Development of Characteristic Qin Medicine Resources (Cultivation), and Shaanxi Collaborative Innovation Center of Chinese Medicinal Resources Industrialization, Shaanxi University of Chinese Medicine, Xi'an 712046, China;* orcid.org/0000-0002-1272-057X; Email: yupingtang@sntcm.edu.cn

Authors

Huan Gao − *Key Laboratory of Shaanxi Administration of Traditional Chinese Medicine for TCM Compatibility, Shaanxi University of Chinese Medicine, Xi'an 712046, China*

Hao-Ming Zhou − *Key Laboratory of Shaanxi Administration of Traditional Chinese Medicine for TCM Compatibility, Shaanxi University of Chinese Medicine, Xi'an 712046, China*

Li-Mei Feng − *Key Laboratory of Shaanxi Administration of Traditional Chinese Medicine for TCM Compatibility, Shaanxi University of Chinese Medicine, Xi'an 712046, China*

Dong-Yan Guo − *Key Laboratory of Shaanxi Administration of Traditional Chinese Medicine for TCM Compatibility, Shaanxi University of Chinese Medicine, Xi'an 712046, China*

Jia-Jia Li − *Key Laboratory of Shaanxi Administration of Traditional Chinese Medicine for TCM Compatibility, Shaanxi University of Chinese Medicine, Xi'an 712046, China*

Qi Zhao − *Key Laboratory of Shaanxi Administration of Traditional Chinese Medicine for TCM Compatibility, Shaanxi University of Chinese Medicine, Xi'an 712046, China*

Lu Huang − *Key Laboratory of Shaanxi Administration of Traditional Chinese Medicine for TCM Compatibility, Shaanxi University of Chinese Medicine, Xi'an 712046, China*

Complete contact information is available at: https://pubs.acs.org/10.1021/acsomega.2c00457

Author Contributions

H.G. contributed to investigation, methodology, formal analysis, and writing of the original draft. H.-M.Z. contributed to validation. S.-J.Y. contributed to conceptualization, methodology, supervision, project administration, funding acquisition, and writing (review and editing). L.-M.F. contributed to formal analysis. D.-Y.G. participated in formal analysis and writing (review and editing). J.-J.L. participated in writing (review and editing). Q.Z. participated in data analysis. L.H. participated in data analysis. Y.-P.T. participated in supervision, methodology, and writing (review and editing).

Funding

This work was supported by the National Natural Science Foundation of China (81903786), the Young Talent Support Program from the Association for Science and Technology of Colleges in Shaanxi Province (20190306), Shaanxi Administration of Traditional Chinese Medicine (2019-ZZ-JC018), Key Research and Development Program of Shaanxi (2019ZDLSF04-05), and Subject Innovation Team of Shaanxi University of Chinese Medicine (2019-YL10).

Notes

The authors declare no competing financial interest.

REFERENCES

(1) Bai, X.; Wang, W. X.; Fu, R. J.; Yue, S. J.; Gao, H.; Chen, Y. Y.; Tang, Y. P. Therapeutic potential of hydroxysafflor yellow A on cardio-cerebrovascular diseases. *Front. Pharmacol.* **2020**, *11*, 1265.

(2) Zhao, F.; Wang, P.; Jiao, Y.; Zhang, X.; Chen, D.; Xu, H. Hydroxysafflor yellow A: A systematical review on botanical resources, physicochemical properties, drug delivery system, pharmacokinetics, and pharmacological effects. *Front. Pharmacol.* **2020**, *11*, 1921.

(3) Wang, S.; Sun, M.; Ping, Q. Enhancing effect of Labrafac Lipophile WL 1349 on oral bioavailability of hydroxysafflor yellow A in rats. *Int. J. Pharm.* **2008**, *358*, 198−204.

(4) Zhang, H. F.; Guo, J. X.; Huang, L. S.; Ping, Q. N. Pharmacokinetics of hydroxysafflor yellow A in rats. *J. China Pharm. Univ* **2006**, *5*, 456−460.

(5) Wu, L.; Kang, A.; Yue, S. J.; Tang, Y. P. Research progress on process of hydroxysafflor yellow A *in vivo*. *Chin. Tradit. Pat. Med.* **2020**, *42*, 150−155.

(6) Liu, F. H.; Ni, W. J.; Yu, S. L.; Huang, A. H.; Zou, J. F.; Li, F. Z. Preparation of hydroxysafflor yellow A phospholipid complex self-microemulsion drug delivery system and its pharmacokinetics in rats. *Chin. J. Mod. Appl. Pharm.* **2021**, *38*, 14−19.

(7) Dai, Y.; van Spronsen, J.; Witkamp, G. J.; Verpoorte, R.; Choi, Y. H. Natural deep eutectic solvents as new potential media for green technology. *Anal. Chim. Acta* **2013**, *766*, 61−68.

(8) Angsantikul, P.; Peng, K.; Curreri, A. M.; Chua, Y.; Chen, K. Z.; Ehondor, J.; Samir, M. Ionic liquids and deep eutectic solvents for enhanced delivery of antibodies in the gastrointestinal tract. *Adv. Funct. Mater.* **2020**, *2020*, 2002912.

(9) Dai, Y.; Witkamp, G. J.; Verpoorte, R.; Choi, Y. H. Natural deep eutectic solvents as a new extraction media for phenolic metabolites in *Carthamus tinctorius* L. *Anal. Chem.* **2013**, *85*, 6272−6278.

(10) Dai, Y.; Verpoorte, R.; Choi, Y. H. Natural deep eutectic solvents providing enhanced stability of natural colorants from safflower (*Carthamus tinctorius*). *Food Chem.* **2014**, *159*, 116−121.

(11) Tong, X.; Yang, J.; Zhao, Y.; Wan, H.; He, Y.; Zhang, L.; Wan, H.; Li, C. Greener extraction process and enhanced *in vivo* bioavailability of bioactive components from *Carthamus tinctorius* L. by natural deep eutectic solvents. *Food Chem.* **2021**, *348*, 129090.

(12) Liu, J.; Yue, S.; Yang, Z.; Feng, W.; Meng, X.; Wang, A.; Peng, C.; Wang, C.; Yan, D. Oral hydroxysafflor yellow A reduces obesity in mice by modulating the gut microbiota and serum metabolism. *Pharmacol. Res.* **2018**, *134*, 40−50.

(13) Nurunnabi, M.; Ibsen, K. N.; Tanner, E. E. L.; Mitragotri, S. Oral ionic liquid for the treatment of diet-induced obesity. *Proc. Natl. Acad. Sci. U. S. A.* **2019**, *116*, 25042−25047.

(14) Boegh, M.; Baldursdóttir, S. G.; Müllertz, A.; Nielsen, H. M. Property profiling of biosimilar mucus in a novel mucus-containing *in vitro* model for assessment of intestinal drug absorption. *Eur. J. Pharm. Biopharm.* **2014**, *87*, 227−235.

(15) Zhang, H. F.; Guo, J. X.; Huang, L. S.; Ping, Q. N. Study on the absorption mechanism of hydroxysafflor yellow A. *J. Beijing Univ. Tradit. Chin. Med.* **2006**, *4*, 312−317.

(16) Zhao, Y. Y.; Fan, Y.; Wang, M.; Wang, J.; Cheng, J. X.; Zou, J. B.; Zhang, X. F.; Shi, Y. J.; Guo, D. Y. Studies on pharmacokinetic properties and absorption mechanism of phloretin: *In vivo* and *in vitro*. *Biomed. Pharmacother.* **2020**, *132*, 110809.

(17) Zhou, W.; Di, L. Q.; Wang, J.; Shan, J. J.; Liu, S. J.; Ju, W. Z.; Cai, B. C. Intestinal absorption of forsythoside A in *in situ* single-pass intestinal perfusion and *in vitro* Caco-2 cell models. *Acta Pharmacol. Sin.* **2012**, *33*, 1069−1079.

(18) Zhang, Y.; Zhang, M.; Hu, G.; Zhang, Z.; Song, R. Elevated system exposures of baicalin after combinatory oral administration of

https://doi.org/10.1021/acsomega.2c00457
ACS Omega 2022, 7, 19225−19234

rhein and baicalin: Mainly related to breast cancer resistance protein (ABCG2), not UDP-glucuronosyltransferases. *J. Ethnopharmacol.* **2020**, *250*, 112528.
(19) Chinese Pharmacopoeia Commission. *Pharmacopoeia of the People's Republic of China Part IV;* China Medical Science Press: Beijing, 2020; pp. 130.
(20) Peng, K.; Gao, Y.; Angsantikul, P.; LaBarbiera, A.; Goetz, M.; Curreri, A. M.; Rodrigues, D.; Tanner, E. E. L.; Mitragotri, S. Modulation of gastrointestinal mucus properties with ionic liquids for drug delivery. *Adv. Healthcare Mater.* **2021**, *10*, 2002192.
(21) Alam, M. A.; Muhammad, G.; Khan, M. N.; Mofijur, M.; Lv, Y.; Xiong, W.; Xu, J. Choline chloride-based deep eutectic solvents as green extractants for the isolation of phenolic compounds from biomass. *J. Cleaner Prod.* **2021**, *309*, 127445.
(22) Doldolova, K.; Bener, M.; Lalikoğlu, M.; Aşcı, Y. S.; Arat, R.; Apak, R. Optimization and modeling of microwave-assisted extraction of curcumin and antioxidant compounds from turmeric by using natural deep eutectic solvents. *Food Chem.* **2021**, *353*, 129337.
(23) Banerjee, A.; Ibsen, K.; Brown, T.; Chen, R.; Agatemor, C.; Mitragotri, S. Ionic liquids for oral insulin delivery. *Proc. Natl. Acad. Sci. U. S. A.* **2018**, *115*, 7296−7301.
(24) Jin, Y.; Wu, L.; Tang, Y. P.; Cao, Y. J.; Li, S. J.; Shen, J.; Yue, S. J.; Qu, C.; Shan, C. X.; Cui, X. B.; Zhang, L.; Duan, J. A. UFLC-Q-TOF/MS based screening and identification of the metabolites in plasma, bile, urine and feces of normal and blood stasis rats after oral administration of hydroxysafflor yellow A. *J. Chromatogr., B* **2016**, *1012*, 124−129.
(25) He, Y.; Su, W.; Chen, T.; Zeng, X.; Yan, Z.; Guo, J.; Yang, W.; Wu, H. Identification of prototype compounds and derived metabolites of naoxintong capsule in beagle dog urine and feces by UFLC-Q-TOF-MS/MS. *J. Pharm. Biomed. Anal.* **2019**, *176*, 112806.
(26) Shearer, J.; Duggan, G.; Weljie, A.; Hittel, D. S.; Wasserman, D. H.; Vogel, H. J. Metabolomic profiling of dietary-induced insulin resistance in the high fat-fed C57BL/6J mouse. *Diabetes, Obes. Metab.* **2008**, *10*, 950−958.
(27) Li, Y.; Zhu, Y. Y.; Shi, L. L.; Shen, L.; Wei, H.; Wang, Y.; Ruan, K. F.; Feng, Y. UPLC-TOF/MS based urinary metabonomic studies reveal mild prevention effects of MDG-1 on metabolic disorders in diet-induced obese mice. *Anal. Methods* **2014**, *6*, 4171−4180.
(28) Schuck, P. F.; Malgarin, F.; Cararo, J. H.; Cardoso, F.; Streck, E. L.; Ferreira, G. C. Phenylketonuria pathophysiology: on the role of metabolic alterations. *Aging Dis.* **2015**, *6*, 390−399.
(29) Adams, S. H. Emerging perspectives on essential amino acid metabolism in obesity and the insulin-resistant state. *Adv. Nutr.* **2011**, *2*, 445−456.
(30) Cervenka, I.; Agudelo, L. Z.; Ruas, J. L. Kynurenines: Tryptophan's metabolites in exercise, inflammation, and mental health. *Science* **2017**, *357*, No. eaaf9794.
(31) Liu, Y.; Hou, Y.; Wang, G.; Zheng, X.; Hao, H. Gut microbial metabolites of aromatic amino acids as signals in host-microbe interplay. *Trends Endocrinol. Metab.* **2020**, *31*, 818−834.
(32) Agus, A.; Planchais, J.; Sokol, H. Gut microbiota regulation of tryptophan metabolism in health and disease. *Cell Host Microbe* **2018**, *23*, 716−724.
(33) Kimura, K.; Nakamura, Y.; Inaba, Y.; Matsumoto, M.; Kido, Y.; Asahara, S.; Matsuda, T.; Watanabe, H.; Maeda, A.; Inagaki, F.; Mukai, C.; Takeda, K.; Akira, S.; Ota, T.; Nakabayashi, H.; Kaneko, S.; Kasuga, M.; Inoue, H. Histidine augments the suppression of hepatic glucose production by central insulin action. *Diabetes* **2013**, *62*, 2266−2277.
(34) Bellissimo, M. P.; Cai, Q.; Ziegler, T. R.; Liu, K. H.; Tran, P. H.; Vos, M. B.; Martin, G. S.; Jones, D. P.; Yu, T.; Alvarez, J. A. Plasma high-resolution metabolomics differentiates adults with normal weight obesity from lean individuals. *Obesity* **2019**, *27*, 1729−1737.

https://doi.org/10.1021/acsomega.2c00457
ACS Omega 2022, 7, 19225−19234